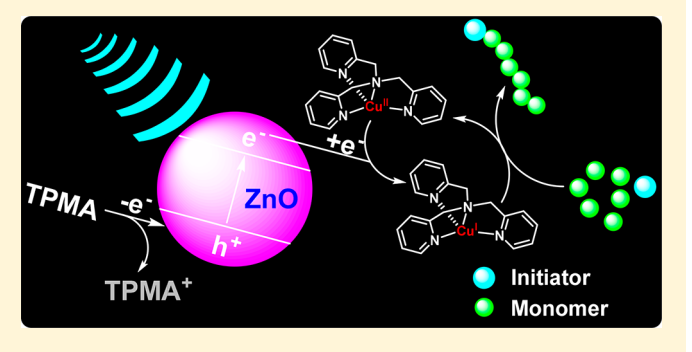
Enhancing Mechanically Induced ATRP by Promoting Interfacial Electron Transfer from Piezoelectric Nanoparticles to Cu Catalysts

Zhenhua Wang,^{†,‡} Xiangcheng Pan,^{‡,§} Lingchun Li,[‡] Marco Fantin,[‡] Jiajun Yan,[‡] Zongyu Wang,[‡] Zhanhua Wang,[†] Hesheng Xia,*,[†] and Krzysztof Matyjaszewski*,[‡]

Supporting Information

ABSTRACT: A robust mechanically controlled atom transfer radical polymerization (mechano-ATRP) was developed by enhancing the interaction between piezoelectric nanoparticles and ATRP Cu catalysts. The interactions favor a mechanoinduced electron transfer from the surface of the nanoparticles to the deactivator Cu^{II}/L complex under ultrasonic agitation, promoting the formation of the activator Cu^I/L complex, thereby increasing the rate of the polymerization. This mechano-ATRP was carried out with a low loading of zinc oxide nanoparticles, providing a polymer with high end-group fidelity, predetermined molecular weight, and low dispersity. Propagation of the polymer chains was switched on/off in



response to the ultrasound. The effects of the nature of the nanoparticle, nanoparticle loading, and targeted degrees of polymerization were investigated to evaluate the mechanism of mechano-ATRP.

■ INTRODUCTION

Stimuli-mediated electron transfer is a powerful protocol in both organic synthesis and polymerization. 1-4 In recent years, various switchable controlled radical polymerization techniques have been developed by manipulating the electron transfer process through external stimuli.^{5,6} This strategy has enabled reversible deactivation radical polymerization with a spatial and temporal control over reaction kinetics, composition, architecture, and functionality. ^{7–9} Photoinduced electron and energy transfer-reversible addition-fragmentation chain transfer polymerization (PET-RAFT) is mediated by photoredox catalysts that can transfer electrons from their excited states to the chaintransfer agents to produce radicals and activate polymerization upon light irradiation. 10–16 Atom transfer radical polymerization (ATRP) is governed by redox-active transition metal complexes in their lower oxidation state (activators) that activate the dormant species and complexes in their higher oxidation state (deactivators) that deactivate the growing radicals. 17-21 This dynamic equilibrium between oxidized and reduced catalyst state can be mediated by various chemical reducing agents, 22-24 electrical current, 7,25,26 or light. 3,9,27-37 Electron transfer (ET) to the deactivator regenerates the activator lost in unavoidable radical termination. It was reported that various semiconductors can be used as electron donor to

initiate the radical polymerization or ATRP under light irradiation.^{38–41}

Mechano-induced electron transfer (MET), which involves the transduction from a mechanical stimulus to an electrical signal, takes part in many biological processes. 42-44 Compared to well-developed PET, MET has been rarely used in controlled radical polymerization. Most recently, a mechanically controlled atom transfer radical polymerization (mechano-ATRP) has been reported in the presence of piezoelectric barium titanate (BTO) particles. ⁴⁵ ET from piezoelectric particles to Cu^{II}/L (L: ligand) was achieved under ultrasonic agitation, generating Cu^I/L to activate the polymerization. Temporal control in mechano-ATRP was achieved using a low ppm of Cu catalyst. 46 However, the reaction required a high loading of piezoelectric barium titanate particles (~4.5 wt %) to maintain the desired polymerization rate throughout the reaction due to the inefficient ET between the nanoparticles and Cu^{II}/L in the heterogeneous system. Stronger interaction between semiconductors and electron acceptors (CuII/L) can favor ET due to decreased energy of the conduction band of the semi-conductor. $^{47-50}$ If $\text{Cu}^{\text{II}}/\text{L}$ is strongly bound to the piezoelectric

Received: July 25, 2017 Revised: September 13, 2017 Published: October 4, 2017

[†]The State Key Laboratory of Polymer Materials Engineering, Polymer Research Institute, Sichuan University, Chengdu 610065,

^{*}Department of Chemistry, Carnegie Mellon University, 4400 Fifth Avenue, Pittsburgh, Pennsylvania 15213, United States §The State Key Laboratory of Molecular Engineering of Polymers, Department of Macromolecular Science, Fudan University, Shanghai 200433, China

nanoparticles, it is anticipated that mechano-induced electrons can be rapidly captured by Cu^{II}/L, resulting in Cu^I/L that can efficiently activate the polymerization. Herein, we demonstrate that MET from piezoelectric nanoparticles to Cu^{II}/L is enhanced by a proper selection of the piezoelectric nanoparticles. ZnO appeared as an excellent candidate. For example, a successful mechano-ATRP can be carried out even at a 0.06 wt % loading of ZnO piezoelectric nanoparticles, a 75-fold decrease as compared to previous results. Efficiencies of bare ZnO and ZnO with solubilizing octylamine (OA) and grafted poly(methyl methacrylate) (PMMA) ligands were compared. The mechano-ATRP technique was used to polymerize several acrylate monomers, with intermittent chain growth in response to ultrasound. The procedure led to well-defined polymers with high end-group fidelity, predetermined molecular weight, and narrow molecular weight distribution (MWD).

EXPERIMENTAL SECTION

Materials. Zinc oxide nanoparticles (18 nm) and barium titanate particles (200 nm, tetragonal) were purchased from US Nano. Ethyl α-bromoisobutyrate (EBiB), copper bromide, and dimethyl sulfoxide (DMSO) were purchased from Aldrich. Tris(2-pyridinylmethyl)amine (TPMA) was synthesized according to previous work. Poly(methyl methacrylate)-stabilized ZnO ($M_{\rm n}=87\,700$, $M_{\rm w}/M_{\rm n}=1.33$, grafting density $\sigma=0.17~{\rm nm}^{-2}$, 41 wt % ZnO) and octylamine-coated ZnO (OA-ZnO, 5 nm) were prepared according to the previous reports. Acrylate monomers were purchased from Aldrich and purified by passing through a column of basic alumina to remove inhibitors. All chemicals were used as received unless otherwise indicated.

Procedures. Procedure for Determining the Evolution of Optical Absorbance of Cu^{II}/L during Ultrasonication. A mixture of CuBr₂ (14.7 mg, 0.066 mmol), TPMA (115 mg, 0.396 mmol), and ZnO (268 mg, 3.3 mmol) or BTO (770 mg, 3.3 mmol) in 20 mL of DMSO was degassed by N₂ purging for 40 min. The resulting suspension was then immersed in an ultrasonic bath equipped with circulating water to keep the reaction temperature at 20–30 °C. At defined time intervals, 1.5 mL aliquots of the suspension were withdrawn and filtered. The resulting filtrate was diluted with 0.3 mL of DMSO, and the absorbance of the solution was measured in a range of 400–1050 nm.

General Procedure for Measuring the Zeta-Potential of Piezo-electric Particles upon Addition of CuBr $_2$ or TPMA. 0.5 mg of BTO or ZnO and 5 mL of DMSO were added to a 20 mL vial. The mixture was exposed to ultrasound for 3 min to give a uniform dispersion. A defined volume of CuBr $_2$ (10 mg/mL) or TPMA (5 mg/mL) in a stock solution was added. After each addition, the resulting mixture was exposed to ultrasound for 3 min. 5 μ L of the above dispersion was withdrawn and diluted with 5 mL of deionized water. The resulting aqueous dispersion was sonicated for 3 min before zeta-potential measurements.

General Procedure for Measuring the Zeta-Potential during Ultrasound. 0.72 mg of CuBr $_2$ (3.2 μ mol, 0.03 equiv), 5.60 mg of TPMA (19.2 μ mol, 0.18 equiv), 0.30 wt % ZnO nanoparticles (12.3 mg), and 4 mL of DMSO were added to a 10 mL Schlenk flask. The flask was bubbled by N $_2$ for 30 min and sealed. The reaction was exposed to the ultrasonic agitation. Samples were withdrawn from the reaction by degassed syringes at timed intervals. 10 μ L of the suspension was diluted with 5 mL of distilled water to give a transparent suspension. The suspension was further sonicated for 3 min to make it stable before zeta-potential measurements.

General Procedure for Mechano-ATRP of Methyl Acrylate. 2 mL of methyl acrylate (MA, 1.9 g, 22 mmol, 200 equiv), 16.2 μ L of EBiB (21.5 mg, 0.11 mmol, 1 equiv), 0.72 mg of CuBr₂ (3.2 μ mol, 0.03 equiv), 5.60 mg of TPMA (19.2 μ mol, 0.18 equiv), 0.30 wt % ZnO nanoparticles (12.3 mg), and 2 mL of DMSO were added to a 10 mL Schlenk flask. The flask was sealed, and the oxygen was removed via three freeze–pump–thaw cycles. The reaction was exposed to ultrasonic agitation. Samples were withdrawn from the reaction by degassed syringes, at timed intervals, to analyze the conversion by 1 H

NMR and by GPC to obtain number-average molecular weight $M_{\rm n}$ and dispersity $(M_{\rm w}/M_{\rm n})$.

Synthesis of a PMA-Br Macroinitiator. 2 mL of MA (1.9 g, 22 mmol, 300 equiv), 10.8 μ L of EBiB (14.4 mg, 0.37 mmol, 1 equiv), 0.48 mg of CuBr₂ (2.13 μ mol, 0.03 equiv), 3.73 mg of TPMA (12.8 μ mol, 0.18 equiv), 0.30 wt % ZnO nanoparticles (8.2 mg), and 2 mL of DMSO were added to a 10 mL Schlenk flask. The flask was sealed and the oxygen was removed via three freeze—pump—thaw cycles. The reaction was exposed to the ultrasonic agitation for 4 h. The reaction was removed from the ultrasonic bath and exposed to air to quench the reaction. 10 mL of THF was added to dilute the reaction mixture which was then passed through neutral Al₂O₃ to remove the ZnO nanoparticles and the Cu^{II} complex. The solvent was then removed by rotavaporation. The macroinitiator was obtained by precipitation in a mixture of MeOH/H₂O (9/1, v/v) and dried under vacuum before further use.

Chain Extension of PMA-Br with MA. 0.2 mL of MA (0.19 g, 2.2 mmol, 300 equiv), 95 mg of macroinitiator (PMA-Br, 0.0073 mmol, 1 equiv), 0.048 mg of CuBr $_2$ (0.213 μ mol, 0.03 equiv), 0.373 mg of TPMA (0.128 μ mol, 0.18 equiv), 0.30 wt % ZnO nanoparticles (0.82 mg), and 0.2 mL of DMSO were added to a 3 mL vial. The vial was sealed, and the oxygen was removed via three freeze–pump—thaw cycles. The reaction was exposed to ultrasonic agitation for 5 h. Samples were withdrawn from the vial to analyze the conversion by 1 H NMR and number-average molecular weight $M_{\rm n}$ and dispersity ($M_{\rm w}/M_{\rm n}$) by GPC with THF as eluent using a linear PMMA standard.

Characterization. ¹H nuclear magnetic resonance (NMR) spectroscopy was performed on a Bruker Avance 300 MHz spectrometer. The molecular weights and dispersities were determined by gel permeation chromatography (GPC). It was equipped with a Waters 515 HPLC pump and a Waters 2414 refractive index detector. PSS columns (SDV 10², 10³, and 10⁵ Å) was used with tetrahydrofuran (THF) as the eluent at a flow rate of 1 mL/min at 35 °C. The apparent molecular weights were determined using linear poly(methyl methacrylate) standards by WinGPC 7.0 software from PSS for the THF GPC. The zeta-potential was measured in a DTS1070 folded capillary zeta cell by a Malvern Zetasizer Nano ZS particle size analyzer. A suspension of nanoparticles in water (0.1 mg/mL), $[CuBr_2] = 0.045$ mM, [TPMA] = 0.28 mM, was used for zetapotential measurements. UV-Vis-IR spectra were measured by an Agilent Cary 60. A photo of the samples was taken by a Canon EOS 5D Mark III digital camera equipped with a Canon EF 100 mm 1:2.8L IS USM Macro lens (f/2.8, 1/100 s, ISO-400) under ambient illumination. The white balance and the exposure were calibrated to a standard 18% gray card in the Canon Digital Photo Professional 4 software. The optical intensities of 10 points on each of the samples, excluding the shadow, were measured using the ImageJ software and normalized. The mechano-induced polymerization was performed in an ultrasonic bath (Fisher Scientific FS 20D, 40 kHz, 70 W); the temperature was kept in a range of 20-30 °C by immersing a hollow Cu cooling coil circulated with running water in the bath. The ultrasonic bath was switched on for 1 h to equilibrate the temperature before conducting a polymerization. The bath was covered by a piece of alumina film to reduce the impact of light on the polymerization.

Cyclic voltammetry was performed on a PARC 273A potentiostat using a three-electrode cell. The working electrode was a glassy carbon disk (3 mm diameter, Metrohm), the counter electrode a Pt wire, and the reference a AglAgIl0.1 M $n\text{-Bu}_4\text{NI}$ in DMF. The reference electrode was separated from the solution by a glass frit and a methylcellulose gel and was calibrated at the end of each experiment against the ferrocenium/ferrocene couple, which has a standard potential of 0.449 V vs SCE. The working electrode was polished with 0.1 μ M alumina paste before each experiment.

■ RESULTS AND DISCUSSION

Piezoelectric ZnO and BTO nanoparticles^{54–56} were selected since they have a similar optical band gap (3.2 eV vs 3.3 eV).⁵⁷ A particle analyzer was used to detect any change of surface charge in the nanoparticles to confirm the interactions between

nanoparticles and CuBr₂/TPMA complexes. Diluted dispersion of piezoelectric particles (0.1 mg/mL) in DMSO were prepared for the measurements because they tended to precipitate at high concentration. Before adding CuBr₂/TPMA (1:6), the ZnO dispersion in water displayed a negative charge ($\xi_{\rm ZnO}$ = -42.7 ± 4.9 mV). The value of $\xi_{\rm ZnO}$ increased to -22.5 ± 5.7 mV upon addition of CuBr₂/TPMA (Figure S1a). However, the values of $\xi_{\rm BTO}$ in water before and after addition of CuBr₂/TPMA were similar, -27.7 ± 4.8 and -31.0 ± 4.2 mV, respectively (Figure S1b). This indicates a weaker interaction between the BTO particles and the catalyst. Moreover, after ultrasonic agitation in the solution of CuBr₂/TPMA, the color of the ZnO nanoparticles became dark gray while the color of BTO remained white (Figure 1a–d), suggesting deposition of

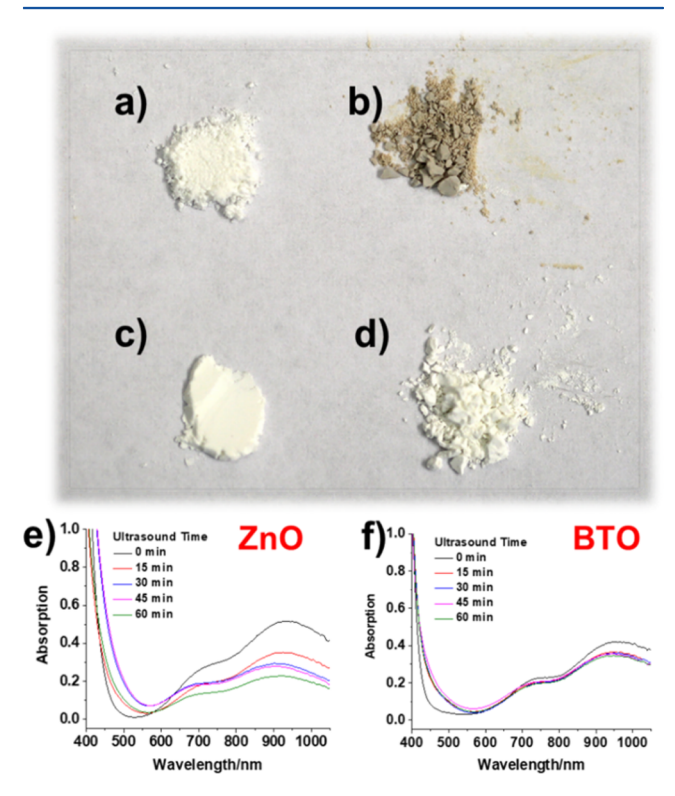


Figure 1. Images of piezoelectric nanoparticles before and after ultrasound agitation in the presence of $CuBr_2/TPMA$ solution: (a) ZnO before ultrasonication; (b) ZnO after ultrasonication; (c) BTO before ultrasonication; (d) BTO after ultrasonication. (e) UV–Vis–NIR spectra with ZnO at different sonication times. (f) UV–Vis–NIR spectra with BTO at different sonication time. Conditions: [$CuBr_2$] = 3.3 mM, [TPMA] = 19.8 mM in DMSO, ZnO 13.4 mg/mL, BTO 38.5 mg/mL. Ultrasound bath (20–30 °C, 40 kHz, 70 W).

Cu species on the ZnO surface. The mechano-induced electron transfer from ZnO or BTO nanoparticles to Cu^{II}/L was further evaluated by UV–Vis–NIR spectra. As ultrasonication proceeded, the optical absorbance of Cu^{II}/L decreased faster in the presence of ZnO, indicating a more efficient electron transfer (Figure 1e,f).

To elucidate the impact of mechano-induced electron transfer, the mechano-ATRP of acrylates was carried out in the presence of either ZnO or BTO nanoparticles under ultrasonic agitation using EBiB as initiator and $\text{CuBr}_2/\text{TPMA}$ as catalyst. The effect of nanoparticles' nature and loading on the ATRP is summarized in Table 1 and Figure 1.

Semilogarithmic kinetic plot in polymerization of methyl acrylate (MA) in the presence of ZnO nanoparticles was linear and polymers with excellent control of molecular weight and low dispersity were obtained. The polymerization with 0.15 wt % ZnO nanoparticles resulted in a conversion of 43% after 8 h, forming a polymer with $M_{\rm n}=8030$ and $M_{\rm w}/M_{\rm n}=1.08$ (entry 1, Table 1). The polymerization rate was proportional to ZnO loading. With 0.60 wt % loading, the polymerization reached 90% conversion after 8 h of ultrasonic agitation, providing a well-defined polymer with $M_{\rm n}=15\,630$ and $M_{\rm w}/M_{\rm n}=1.06$ (entry 3, Table 1). No conversion was observed in the control experiment without ultrasonication (entry 3, Table S1), indicating that there was no photoreduction of Cu^{II} under the standard conditions.

The polymerization with 0.30 wt % PMMA-stabilized ZnO resulted in higher conversion after 8 h ultrasonication (78%, entry 4, Table 1) compared to the reaction with pure ZnO (70%, entry 2, Table 1). This could be attributed to lower degree of aggregation of the PMMA–ZnO under ultrasonication. With PMMA–ZnO the loading of the piezoelectric nanoparticles was further reduced to 0.10 wt % (entry 5, Table 1).

Smaller nanoparticles, with a dispersant on their surface, can be used to obtain a transparent polymerization media. This could be useful, for example, to control polymerization with multiple stimuli, mechanical energy and light. The polymerization mixture with 0.06 wt % OA–ZnO (5 nm diameter) was transparent and reached 75% conversion after 8 ultrasonication, giving a polymer with $M_{\rm n}=12\,890$ and $M_{\rm w}/M_{\rm n}=1.08$ (entry 6, Table 1).

In the presence of 0.9 wt % BTO, a much lower conversion (~4%) was obtained after 8 h of ultrasonication (entry 7, Table 1). The conversion increased to 61% in the presence of 4.5 wt % BTO (entry 9, Table 1). These results indicate that ZnO promoted more efficient mechano-induced electron transfer, producing a higher concentration of activator. In the case of BTO nanoparticles, a higher loading was required to achieve an acceptable rate of polymerization due to weaker interactions between the nanoparticles and CuBr₂/TPMA catalyst complex.

The mechano-ATRP technique was also extended to the polymerization of other acrylates including ethyl acrylate, butyl acrylate, and *tert*-butyl acrylate (entries 1–3, Table 2). All polymerizations were well-controlled with predictable molecular weights and narrow molecular weight distributions. The polymerization of methyl methacrylate was less controlled using EBiB as initiator, plausibly due to lower reactivity of initiator than growing chains, due to the penultimate unit effect (entry 4, Table 2). No conversion was observed in the absence of either TPMA or ZnO after 8 h ultrasonication (entries 3 and 4, Table S1), indicating their critical role in the generation of activators for an ATRP.

Mechanistic Investigation. Four pathways for the activator generation were considered. The first pathway is the ultrasound-induced ET from ZnO nanoparticles to the deactivator (Cu^{II}/L). As confirmed by UV-Vis-NIR spectra (Figure 1), under ultrasonic agitation ZnO nanoparticles can reduce Cu^{II} to Cu^{II} species. To maintain electron neutrality, an oxidation reaction must concurrently happen, i.e., filling the positive electron hole generated in the ZnO nanoparticles. This oxidation process did not generate of initiating radicals because the experimental molecular weights agreed well with the theoretical values, indicating a constant number of propagating chains, corresponding to the initial number of initiators (alkyl

Table 1. Results	for Mechano-ATRP	of Methyl Acrylate
------------------	------------------	--------------------

entry ^a	piezoelectric particles	loading (wt %)	time (h)	$conv^b$ (%)	$M_{ m n,th}^{c}$	$M_{ m n,GPC}^{d}$	$M_{\rm w}/M_{\rm n}^{}$
1	ZnO (18 nm)	0.15	8	43	7590	8030	1.08
2	ZnO (18 nm)	0.30	8	70	12240	13500	1.06
3	ZnO (18 nm)	0.60	8	90	15680	15630	1.06
4	PMMA-ZnO (18 nm)	0.10	8	53	10450	9310	1.07
5	PMMA-ZnO (18 nm)	0.30	8	78	13000	13600	1.07
6	OA-ZnO (5 nm)	0.06	8	75	13100	12890	1.08
7	BTO (200 nm)	0.90	8	4	N/A	N/A	N/A
8	BTO (200 nm)	1.80	8	30	5350	4960	1.12
9	BTO (200 nm)	4.50	8	61	9800	9130	1.08

^aReaction conditions: [MA]₀:[EBiB]₀:[CuBr₂]₀:[TPMA]₀ = 200:1:0.03:0.18 in 50% (v/v) DMSO; loading of piezoelectric particles was expressed with respect to the mass of all the reagents including MA, EBiB, CuBr₂, TPMA, and DMSO. Ultrasonic bath (20–30 °C, 40 kHz, 70 W). ^bConversion determined by ¹H NMR. ^cCalculated on the basis of conversion (i.e., $M_{\rm n,th} = M_{\rm EBiB} + [\rm MA]_0/[EBiB]_0 \times {\rm conversion} \times M_{\rm monomer}$). ^dDetermined by GPC in THF, based on linear PMMA as calibration standard.

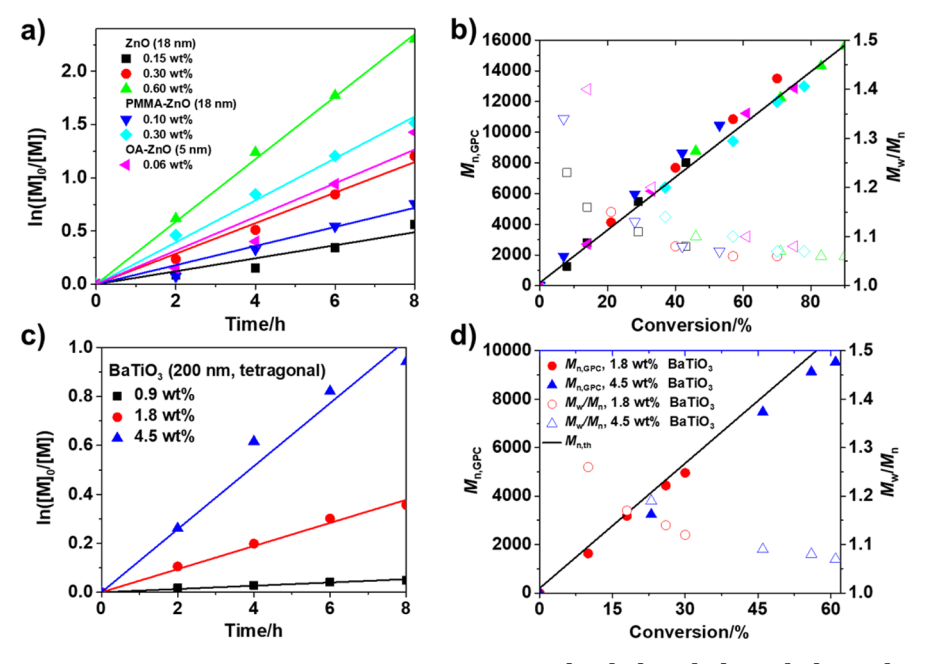


Figure 2. Results for polymerization of MA by mechano-ATRP under conditions $[MA]_0/[EBiB]_0/[CuBr_2]_0/[TPMA]_0 = 200/1/0.03/0.18$ with various loadings of ZnO and BTO nanoparticles in 50% (v/v) dimethyl sulfoxide (DMSO), ultrasound bath (20–30 °C, 40 kHz, 70 W). (a) Semilogarithmic kinetic plots for ZnO systems and (b) number-average molecular weight and molecular weight distribution (M_w/M_n) for ZnO systems. (c) Semilogarithmic kinetic plots for BTO systems and (d) number-average molecular weight and molecular weight distribution (M_w/M_n) for BTO systems.

Table 2. Results for Mechano-ATRP of Various Acrylates Using ZnO Nanoparticles

entry ^a	monomer	loading of ZnO (wt %) (18 nm)	time (h)	conv ^b (%)	$M_{ m n,th}^{c}$	$M_{ m n,GPC}^{d}$	$M_{\rm w}/{M_{ m n}}^d$
1	EA	0.60	6	80	16200	18760	1.06
2 ^e	tBA	0.60	12	71	18370	19450	1.12
3 ^e	BA	0.60	12	65	16830	17820	1.08
4	MMA	0.60	15	36	7400	12090	1.24

"Reaction conditions: [M]₀:[EBiB]₀:[CuBr₂]₀:[TPMA]₀ = 200:1:0.03:0.18 in 50% (v/v) DMSO, ZnO (18 nm), ultrasonic bath (20–30 °C, 40 kHz, 70 W). "Conversion determined by ¹H NMR. "Calculated on the basis of conversion (i.e., $M_{\rm n,th} = M_{\rm EBiB} + [{\rm MA}]_0/[{\rm EBiB}]_0 \times {\rm conversion} \times M_{\rm monomer}$). "Determined by GPC in THF, based on linear PMMA as calibration standard. "Polymerization was conducted in DMF.

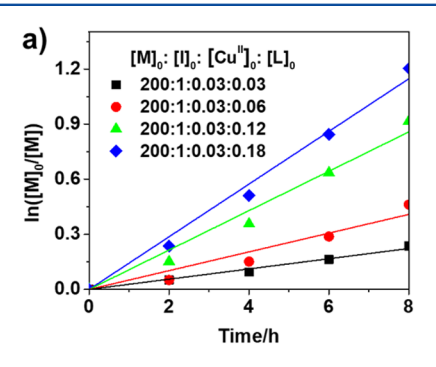
halides). Cyclic voltammetry (CV) curves were recorded to investigate the redox behavior of the reagents in the reaction. As revealed in Figure S2, the oxidation potential of TPMA (+1.04 V vs SCE) is much lower than that of DMSO (+1.54 V vs SCE). Therefore, it is plausible that TPMA serves as the sacrificial electron donor in this system. Because TPMA can coordinate to Zn^{2+,60} some free ligand molecules attached to the surface of ZnO nanoparticles can facilitate the electron

transfer from TPMA to stabilize the hole. Zeta-potential was recorded during the reduction of Cu^{II} under ultrasonication (Figure S1d). The value of ξ_{ZnO} remained almost constant as ultrasonication proceeded, indicating the charge was well balanced and the positive hole was filled. This was further supported by the results of polymerizations using various ratio of $CuBr_2/TPMA$ (Table 2), specifically the polymerization with 1:1 molar ratio of $CuBr_2/TPMA$ displayed inferior control

Table 3. Results for Mechano-ATRP of MA with Different Concentrations of TPMA

entry ^a	conditions ([M] $_0$ /[I] $_0$ /[Cu $^{\rm II}$] $_0$ /[L] $_0$)	ZnO (wt %) (18 nm)	time (h)	$conv^b$ (%)	$M_{ m n,th}^{c}$	$M_{ m n,GPC}^{d}$	$M_{\rm w}/M_{\rm n}^{}$
1	200:1:0.03:0.03	0.30	8	21	3800	4520	1.77
2	200:1:0.03:0.06	0.30	8	37	6560	7700	1.09
3	200:1:0.03:0.12	0.30	8	60	10520	12560	1.06
4	200:1:0.03:0.18	0.30	8	70	12240	13500	1.06

"Reaction conditions: 50% (v/v) DMSO, 0.30 wt % ZnO (18 nm), ultrasound bath (20–30 °C, 40 kHz, 70 W). Conversion determined by 1 H NMR. Calculated on the basis of conversion (i.e., $M_{\rm n,th} = M_{\rm EBiB} + [{\rm MA}]_{\rm 0}/[{\rm EBiB}]_{\rm 0} \times {\rm conversion} \times M_{\rm monomer}$). Determined by GPC in THF, based on linear PMMA as calibration standard.



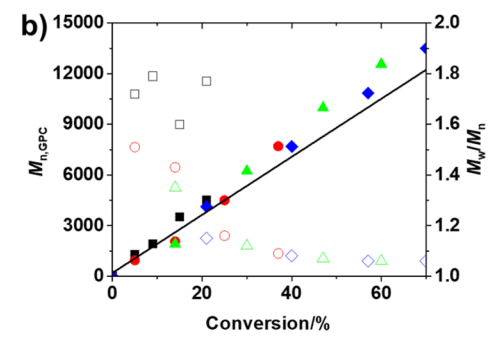
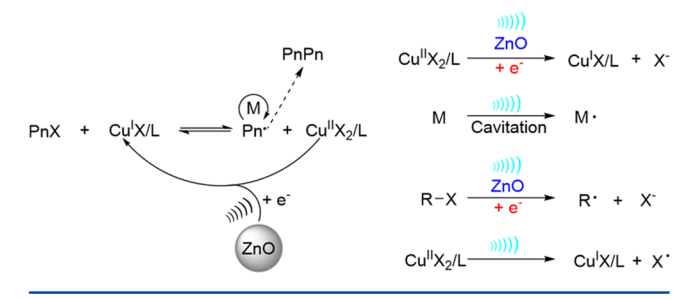


Figure 3. Results for the polymerization of MA in the presence various concentration of TMPA. (a) Kinetics and (b) molecular weight and dispersity of polymers. Reaction conditions: $[MA]_0$: $[EBiB]_0$: $[CuBr_2]_0$: $[TPMA]_0 = 200:1:0.03:X$, 0.30 wt % ZnO, in 50% (v/v) DMSO (20–30 °C, 40 kHz, 70 W).

 $(M_{\rm w}/M_{\rm n} > 1.6)$ (entry 1, Table 3), indicating that a fraction of TPMA ligand was consumed during the ultrasonication, diminishing the amount of ${\rm CuBr_2}/{\rm TPMA}$ catalyst complex in the reaction. Faster polymerization and better control were attained at higher TPMA concentration, as shown in Figure 3.

The second pathway (Scheme 1) for activation of the catalyst could be formation of radicals from monomer/solvent by

Scheme 1. Proposed Mechanism of Mechano-ATRP and Pathways of Activator Generation



cavitation which could initiate new chains. The polymerization in the absence of CuBr₂/TPMA and EBiB after 8 h ultrasonication resulted in low conversion (<15%) generating a polymer with high molecular weight $(M_n > 260000)$ and broad molecular weight distribution $(M_w/M_n > 1.9)$ (Table S1). Indeed, ultrasonication can induce free radical polymerization of acrylates but requires continuous nitrogen or argon flow to maintain the concentration of nuclei for cavitation in order to achieve a sufficient conversion. 61-63 The actual contribution of radicals from cavitation to the mechano-ATRP is limited because polymerization reached a very low conversion (<5%) in the absence of EBiB (entry 1, Table S1). Furthermore, to confirm that most polymer chains originated from EBiB, mechano-ATRP of MA targeting various degrees of polymerization (DP) were conducted and the results are summarized in Table 4. The monomer concentration was kept

Table 4. Results for Mechano-ATRP of Acrylates with Various DP_{T}

entrya	conditions $([M]_0/[I]_0/[Cu^{II}]_0/[L]_0)$	time (h)	conv ^b (%)	$M_{ m n,th}^{c}$	$M_{ m n,GPC}^{d}$	$M_{ m w}/M_{ m n}^{d}$
1	50:1:0.03:0.18	6	83	3760	3870	1.08
2	100:1:0.03:0.18	6	65	5790	5670	1.08
3	200:1:0.03:0.18	8	70	12240	13500	1.06
4	300:1:0.03:0.18	8	74	19290	17190	1.07
5	400:1:0.03:0.18	4	39	13610	12890	1.09
6 ^e	200:1:0.03:0.18	12	65	16830	17820	1.08
7^e	400:1:0.03:0.18	16	65	33470	30350	1.15

"Reaction conditions: 50% (v/v) DMSO, 0.30 wt % ZnO (18 nm), ultrasound bath (20–30 °C, 40 kHz, 70 W). ^bConversion determined by ¹H NMR. ^cCalculated on the basis of conversion (i.e., $M_{\rm n,th}=M_{\rm EBiB}+[{\rm MA}]_0/[{\rm EBiB}]_0 \times {\rm conversion}\times M_{\rm monomer})$. ^dDetermined by GPC in THF, based on linear PMMA as calibration standard. ^eButyl acrylate as monomer, DMF as solvent, with 0.6 wt % ZnO.

constant in all reactions, while the concentrations of EBiB, CuBr₂, and TPMA were varied with respect to the targeted DP (DP_T) . Polymerization of MA with $DP_T = 50$ reached a conversion of 83% to give PMA with $M_n = 3870$ and a low dispersity of 1.08 after 6 h of ultrasonic agitation (entry 1, Table 4). The polymerization with $DP_T = 100$ resulted in 65% conversion, giving a polymer with $M_{\rm n}$ = 5670 and $M_{\rm w}/M_{\rm n}$ = 1.08 (entry 2, Table 4). The conversion reached 70% after 8 h when $DP_T = 200$ (entry 3, Table 4). Polymerization of MA with $DP_T = 300$ reached a conversion of 74% to form PMA with $M_{\rm n}$ = 19 290 and a low dispersity of 1.07 (entry 4, Table 4). The polymerization of BA targeting $DP_T = 200$ and $DP_T =$ 400 reached 65% after 12 and 16 h, respectively (entries 6 and 7, Table 4). These results demonstrated that almost all the polymers were grown from EBiB as the experimental molecular weights agreed well with theoretical values along with generation of polymers with narrow molecular weight distributions.

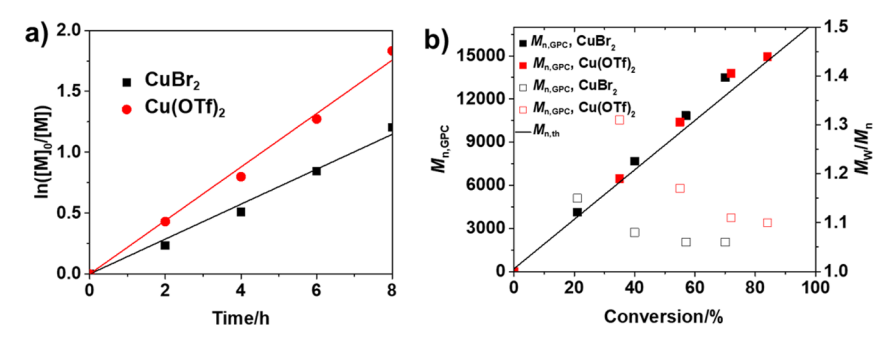


Figure 4. Results for polymerization of MA by mechano-ATRP under conditions $[MA]_0/[EBiB]_0/[Cu^{II}]_0/[TPMA]_0 = 200/1/0.03/0.18$, 0.30 wt % ZnO in 50% (v/v) DMSO, ultrasound bath (20–30 °C, 40 kHz, 70 W). (a) Semilogarithmic kinetic plots and (b) evolution of number-average molecular weight and molecular weight distribution (M_w/M_n) .

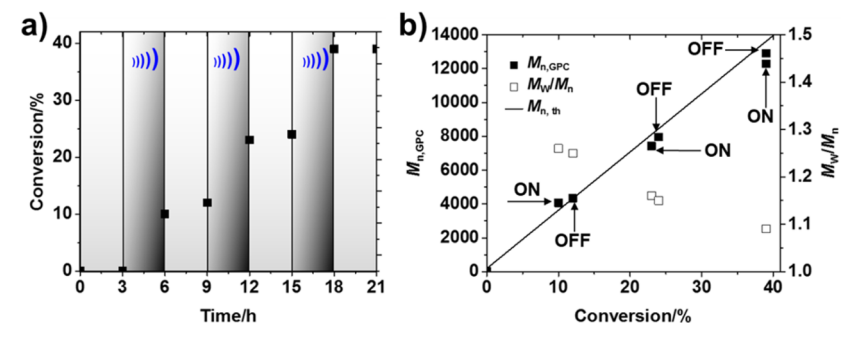


Figure 5. Evidence of temporal control in mechano-ATRP with a low loading of ZnO nanoparticles under ultrasound agitation through intermittent switching on/off ultrasound bath $(20-30 \, ^{\circ}\text{C}, 40 \, \text{kHz}, 70 \, \text{W})$. (a) Kinetics and (b) molecular weight and dispersity of polymers. Reaction conditions: $[MA]_0$: $[EBiB]_0$: $[CuBr_2]_0$: $[TPMA]_0 = 400:1:0.03:0.18$, 0.15 wt % ZnO (18 nm), in 50% (v/v) DMSO.

The third possibility for the activator generation shown in Scheme 1 was the direct reduction of alkyl halide to form carbon radicals by ZnO nanoparticles under ultrasonication. This pathway was excluded because ¹H NMR spectra of EBiB remained unchanged after 7 h ultrasonication in the presence of ZnO nanoparticles (Figure S3), indicating ZnO nanoparticles cannot efficiently directly reduce EBiB under ultrasonication.

The last pathway shown in Scheme 1 was the homolytic cleavage of the TPMA/Cu^{II}-halogen bond. Therefore, a reaction was carried out using copper(II) triflate (Cu(OTf)₂) instead of CuBr₂. In both reactions, the ratio of [Cu^{II}]₀: [TPMA]₀ was 1:6. There was no halide initially bound to Cu^{II} in the Cu(OTf)₂ system. Thus, if homolytic cleavage of the Cu^{II}-halogen bond dominated the reduction process, the polymerization would be much slower than the reaction with CuBr₂. However, as shown in Figure 4, the polymerization with Cu(OTf)₂ was actually faster than the reaction with CuBr₂, suggesting that the homolytic cleavage of the Cu^{II}-halogen bond did not contribute to the activation of the catalyst. The faster polymerization rate should be due to the faster reduction of Cu(OTf)₂/TPMA, which has a more positive standard reduction potential than CuBr₂/TPMA.⁶⁴ This result further corroborates the predominant role of ZnO as the reducing agent of CuBr₂/TPMA under sonication, as illustrated in a pathway 1 in Scheme 1.

Switchable Polymerization in Response to Ultrasonication. Polymerization can be reversibly switched "off" or "on" in response to ultrasound as shown in Figure 5a. A low conversion was attained in the absence of ultrasound, while a steady continuation of the polymer chain growth was obtained after re-exposure to the ultrasonic agitation. Additionally, excellent control over the polymerization was achieved as confirmed by polymers with low dispersity and molecular weights close to theoretical values (Figure 5b).

To confirm retention of chain-end functionality in the mechano-ATRP procedure, chain extension of the initially formed PMA-Br was carried out. The polymerization was conducted under typical conditions and provided a PMA-Br macroinitiator with $M_{\rm n}=11\,380$ and $M_{\rm w}/M_{\rm n}=1.08$ at 52% conversion. After precipitation and purification, the macroinitiator was obtained. Chain extension of PMA-Br was conducted under typical procedures. After 5 h of ultrasonic agitation, the chain-extended polymerization reached 46% conversion, giving PMA-b-PMA-Br with $M_{\rm n}=24\,390$ and $M_{\rm w}/M_{\rm n}=1.10$ (Figure 6).

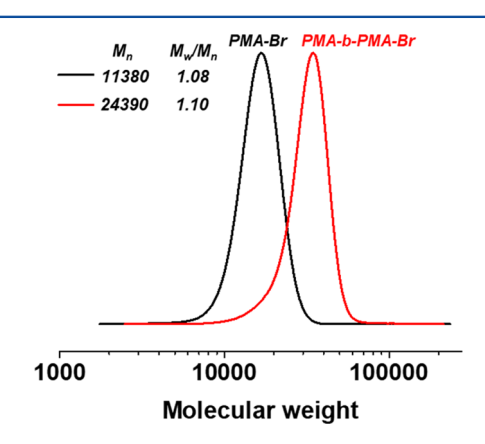


Figure 6. GPC traces of PMA-Br (black) and PMA-b-PMA-Br (red).

CONCLUSIONS

A robust mechano-ATRP was developed in the presence of low loading of ZnO particles. Enhanced interfacial interactions between ZnO nanoparticles and a Cu^{II} catalyst complex enabled a polymerization resulting in 90% conversion after 8 h of ultrasonic agitation. The results demonstrated that the dominant mode of activator regeneration was the mechanically induced electron transfer from ZnO nanoparticles to the deactivator Cu^{II} species. This mechanochemical process involved the reduction of Cu^{II} into Cu^I to activate the polymerization and oxidation of excess TPMA to balance the charge. A second, less significant, step was radical generation by the ultrasound-induced cavitation.

This mechano-ATRP technique was applied to polymerization of several (meth)acrylates, yielding well-defined polymers with high end-group fidelity, predetermined molecular weight, and narrow molecular weight distribution. The polymerization can be temporally controlled by intermittent switching off the ultrasonic bath.

ASSOCIATED CONTENT

S Supporting Information

The Supporting Information is available free of charge on the ACS Publications website at DOI: 10.1021/acs.macromol.7b01597.

CV curves of reagents used in our experiments, a table of the control experiments, zeta-potential of ZnO nanoparticles during ultrasound, ¹H NMR spectra of EBiB before/after ultrasound (PDF)

AUTHOR INFORMATION

Corresponding Authors

*(H.X.) E-mail xiahs@scu.edu.cn.

*(K.M.) E-mail km3b@andrew.cmu.edu.

ORCID ®

Zhenhua Wang: 0000-0002-9028-6799 Xiangcheng Pan: 0000-0003-3344-4639 Lingchun Li: 0000-0003-2122-5201 Jiajun Yan: 0000-0003-3286-3268 Zhanhua Wang: 0000-0003-0493-1905

Krzysztof Matyjaszewski: 0000-0003-1960-3402

Notes

The authors declare no competing financial interest.

ACKNOWLEDGMENTS

We thank the NSF (CHE-1707490) for financial support. H.X. acknowledges the National Natural Science Foundation of China (51473094). X.P. acknowledges the National Natural Science Foundation of China (21704017). Z.W. gratefully acknowledges financial support from China Scholarship Council.

REFERENCES

- (1) Piermattei, A.; Karthikeyan, S.; Sijbesma, R. P. Activating catalysts with mechanical force. *Nat. Chem.* **2009**, *1*, 133–137.
- (2) Shaw, M. H.; Twilton, J.; MacMillan, D. W. C. Photoredox Catalysis in Organic Chemistry. J. Org. Chem. 2016, 81, 6898–6926.
- (3) Pan, X.; Tasdelen, M. A.; Laun, J.; Junkers, T.; Yagci, Y.; Matyjaszewski, K. Photomediated controlled radical polymerization. *Prog. Polym. Sci.* **2016**, *62*, 73–125.

- (4) Chen, M.; Zhong, M.; Johnson, J. A. Light-Controlled Radical Polymerization: Mechanisms, Methods, and Applications. *Chem. Rev.* **2016**, *116*, 10167–10211.
- (5) Leibfarth, F. A.; Mattson, K. M.; Fors, B. P.; Collins, H. A.; Hawker, C. J. External Regulation of Controlled Polymerizations. *Angew. Chem., Int. Ed.* **2013**, 52, 199–210.
- (6) Teator, A. J.; Lastovickova, D. N.; Bielawski, C. W. Switchable Polymerization Catalysts. *Chem. Rev.* **2016**, *116*, 1969–1992.
- (7) Magenau, A. J. D.; Strandwitz, N. C.; Gennaro, A.; Matyjaszewski, K. Electrochemically Mediated Atom Transfer Radical Polymerization. *Science* **2011**, 332, 81–84.
- (8) Fors, B. P.; Hawker, C. J. Control of a Living Radical Polymerization of Methacrylates by Light. *Angew. Chem., Int. Ed.* **2012**, *51*, 8850–8853.
- (9) Treat, N. J.; Sprafke, H.; Kramer, J. W.; Clark, P. G.; Barton, B. E.; Read de Alaniz, J.; Fors, B. P.; Hawker, C. J. Metal-Free Atom Transfer Radical Polymerization. *J. Am. Chem. Soc.* **2014**, *136*, 16096—16101.
- (10) Xu, J.; Jung, K.; Atme, A.; Shanmugam, S.; Boyer, C. A Robust and Versatile Photoinduced Living Polymerization of Conjugated and Unconjugated Monomers and Its Oxygen Tolerance. *J. Am. Chem. Soc.* **2014**, *136*, 5508–5519.
- (11) Xu, J.; Jung, K.; Boyer, C. Oxygen Tolerance Study of Photoinduced Electron Transfer—Reversible Addition—Fragmentation Chain Transfer (PET-RAFT) Polymerization Mediated by Ru(bpy)₃Cl₂. *Macromolecules* **2014**, *47*, 4217–4229.
- (12) Shanmugam, S.; Xu, J.; Boyer, C. Utilizing the electron transfer mechanism of chlorophyll a under light for controlled radical polymerization. *Chem. Sci.* **2015**, *6*, 1341–1349.
- (13) Shanmugam, S.; Xu, J.; Boyer, C. Aqueous RAFT Photopolymerization with Oxygen Tolerance. *Macromolecules* **2016**, *49*, 9345–9357.
- (14) Chen, M.; Deng, S.; Gu, Y.; Lin, J.; MacLeod, M. J.; Johnson, J. A. Logic-Controlled Radical Polymerization with Heat and Light: Multiple-Stimuli Switching of Polymer Chain Growth via a Recyclable, Thermally Responsive Gel Photoredox Catalyst. *J. Am. Chem. Soc.* 2017, 139, 2257–2266.
- (15) Xu, J.; Shanmugam, S.; Fu, C.; Aguey-Zinsou, K.-F.; Boyer, C. Selective Photoactivation: From a Single Unit Monomer Insertion Reaction to Controlled Polymer Architectures. *J. Am. Chem. Soc.* **2016**, 138, 3094–3106.
- (16) Xu, J.; Fu, C.; Shanmugam, S.; Hawker, C. J.; Moad, G.; Boyer, C. Synthesis of Discrete Oligomers by Sequential PET-RAFT Single-Unit Monomer Insertion. *Angew. Chem., Int. Ed.* **2017**, *56*, 8376–8383.
- (17) Kato, M.; Kamigaito, M.; Sawamoto, M.; Higashimura, T. Polymerization of Methyl Methacrylate with the Carbon Tetrachloride/Dichlorotris- (triphenylphosphine)ruthenium(II)/Methylaluminum Bis(2,6-di-tert-butylphenoxide) Initiating System: Possibility of Living Radical Polymerization. *Macromolecules* 1995, 28, 1721–1723.
- (18) Wang, J.-S.; Matyjaszewski, K. Controlled/"living" radical polymerization. atom transfer radical polymerization in the presence of transition-metal complexes. *J. Am. Chem. Soc.* **1995**, *117*, 5614–5615.
- (19) Matyjaszewski, K.; Xia, J. Atom Transfer Radical Polymerization. *Chem. Rev.* **2001**, *101*, 2921–2990.
- (20) Matyjaszewski, K. Atom Transfer Radical Polymerization (ATRP): Current Status and Future Perspectives. *Macromolecules* **2012**, *45*, 4015–4039.
- (21) Matyjaszewski, K.; Tsarevsky, N. V. Macromolecular Engineering by Atom Transfer Radical Polymerization. *J. Am. Chem. Soc.* **2014**, 136, 6513–6533.
- (22) Kwak, Y.; Magenau, A. J. D.; Matyjaszewski, K. ARGET ATRP of Methyl Acrylate with Inexpensive Ligands and ppm Concentrations of Catalyst. *Macromolecules* **2011**, *44*, 811–819.
- (23) Konkolewicz, D.; Magenau, A. J. D.; Averick, S. E.; Simakova, A.; He, H.; Matyjaszewski, K. ICAR ATRP with ppm Cu Catalyst in Water. *Macromolecules* **2012**, *45*, 4461–4468.
- (24) Konkolewicz, D.; Wang, Y.; Zhong, M.; Krys, P.; Isse, A. A.; Gennaro, A.; Matyjaszewski, K. Reversible-Deactivation Radical

Polymerization in the Presence of Metallic Copper. A Critical Assessment of the SARA ATRP and SET-LRP Mechanisms. *Macromolecules* **2013**, *46*, 8749–8772.

- (25) Park, S.; Chmielarz, P.; Gennaro, A.; Matyjaszewski, K. Simplified Electrochemically Mediated Atom Transfer Radical Polymerization using a Sacrificial Anode. *Angew. Chem., Int. Ed.* **2015**, *54*, 2388–2392.
- (26) Chmielarz, P.; Fantin, M.; Park, S.; Isse, A. A.; Gennaro, A.; Magenau, A. J. D.; Sobkowiak, A.; Matyjaszewski, K. Electrochemically mediated atom transfer radical polymerization (eATRP). *Prog. Polym. Sci.* **2017**, *69*, 47–78.
- (27) Konkolewicz, D.; Schröder, K.; Buback, J.; Bernhard, S.; Matyjaszewski, K. Visible Light and Sunlight Photoinduced ATRP with ppm of Cu Catalyst. ACS Macro Lett. 2012, 1, 1219–1223.
- (28) Anastasaki, A.; Nikolaou, V.; Zhang, Q.; Burns, J.; Samanta, S. R.; Waldron, C.; Haddleton, A. J.; McHale, R.; Fox, D.; Percec, V.; Wilson, P.; Haddleton, D. M. Copper(II)/Tertiary Amine Synergy in Photoinduced Living Radical Polymerization: Accelerated Synthesis of ω -Functional and α , ω -Heterofunctional Poly(acrylates). *J. Am. Chem. Soc.* **2014**, *136*, 1141–1149.
- (29) Ribelli, T. G.; Konkolewicz, D.; Bernhard, S.; Matyjaszewski, K. How are Radicals (Re)Generated in Photochemical ATRP? *J. Am. Chem. Soc.* **2014**, *136*, 13303–13312.
- (30) Pan, X.; Lamson, M.; Yan, J.; Matyjaszewski, K. Photoinduced Metal-Free Atom Transfer Radical Polymerization of Acrylonitrile. *ACS Macro Lett.* **2015**, *4*, 192–196.
- (31) Pan, X.; Malhotra, N.; Simakova, A.; Wang, Z.; Konkolewicz, D.; Matyjaszewski, K. Photoinduced Atom Transfer Radical Polymerization with ppm-Level Cu Catalyst by Visible Light in Aqueous Media. J. Am. Chem. Soc. 2015, 137, 15430—15433.
- (32) Pan, X.; Malhotra, N.; Zhang, J.; Matyjaszewski, K. Photo-induced Fe-Based Atom Transfer Radical Polymerization in the Absence of Additional Ligands, Reducing Agents, and Radical Initiators. *Macromolecules* **2015**, *48*, 6948–6954.
- (33) Pan, X.; Fang, C.; Fantin, M.; Malhotra, N.; So, W. Y.; Peteanu, L. A.; Isse, A. A.; Gennaro, A.; Liu, P.; Matyjaszewski, K. Mechanism of Photoinduced Metal-Free Atom Transfer Radical Polymerization: Experimental and Computational Studies. *J. Am. Chem. Soc.* **2016**, *138*, 2411–2425.
- (34) Pan, X.; Lathwal, S.; Mack, S.; Yan, J.; Das, S. R.; Matyjaszewski, K. Automated Synthesis of Well-Defined Polymers and Biohybrids by Atom Transfer Radical Polymerization Using a DNA Synthesizer. *Angew. Chem., Int. Ed.* **2017**, *56*, 2740–2743.
- (35) Discekici, E. H.; Anastasaki, A.; Kaminker, R.; Willenbacher, J.; Truong, N. P.; Fleischmann, C.; Oschmann, B.; Lunn, D. J.; Read de Alaniz, J.; Davis, T. P.; Bates, C. M.; Hawker, C. J. Light-Mediated Atom Transfer Radical Polymerization of Semi-Fluorinated (Meth)acrylates: Facile Access to Functional Materials. *J. Am. Chem. Soc.* 2017, 139, 5939–5945.
- (36) Theriot, J. C.; Lim, C.-H.; Yang, H.; Ryan, M. D.; Musgrave, C. B.; Miyake, G. M. Organocatalyzed atom transfer radical polymerization driven by visible light. *Science* **2016**, 352, 1082–1086.
- (37) Ryan, M. D.; Pearson, R. M.; French, T. A.; Miyake, G. M. Impact of Light Intensity on Control in Photoinduced Organocatalyzed Atom Transfer Radical Polymerization. *Macromolecules* **2017**, 50, 4616–4622.
- (38) Zhang, D.; Yang, J.; Bao, S.; Wu, Q.; Wang, Q. Semiconductor nanoparticle-based hydrogels prepared via self-initiated polymerization under sunlight, even visible light. *Sci. Rep.* **2013**, *3*, 1399.
- (39) Dadashi-Silab, S.; Atilla Tasdelen, M.; Mohamed Asiri, A.; Bahadar Khan, S.; Yagci, Y. Photoinduced Atom Transfer Radical Polymerization Using Semiconductor Nanoparticles. *Macromol. Rapid Commun.* **2014**, *35*, 454–459.
- (40) Dadashi-Silab, S.; Tasdelen, M. A.; Kiskan, B.; Wang, X.; Antonietti, M.; Yagci, Y. Photochemically Mediated Atom Transfer Radical Polymerization Using Polymeric Semiconductor Mesoporous Graphitic Carbon Nitride. *Macromol. Chem. Phys.* **2014**, *215*, 675–681.
- (41) Kiskan, B.; Zhang, J.; Wang, X.; Antonietti, M.; Yagci, Y. Mesoporous Graphitic Carbon Nitride as a Heterogeneous Visible

Light Photoinitiator for Radical Polymerization. *ACS Macro Lett.* **2012**, 1, 546–549.

- (42) French, A. S. Mechanotransduction. Annu. Rev. Physiol. 1992, 54, 135-152.
- (43) Caruso, M. M.; Davis, D. A.; Shen, Q.; Odom, S. A.; Sottos, N. R.; White, S. R.; Moore, J. S. Mechanically-Induced Chemical Changes in Polymeric Materials. *Chem. Rev.* **2009**, *109*, *5755*–*5798*.
- (44) Ross, T. D.; Coon, B. G.; Yun, S.; Baeyens, N.; Tanaka, K.; Ouyang, M.; Schwartz, M. A. Integrins in mechanotransduction. *Curr. Opin. Cell Biol.* **2013**, 25, 613–618.
- (45) Mohapatra, H.; Kleiman, M.; Esser-Kahn, A. P. Mechanically controlled radical polymerization initiated by ultrasound. *Nat. Chem.* **2016**, *9*, 135–139.
- (46) Wang, Z.; Pan, X.; Yan, J.; Dadashi-Silab, S.; Xie, G.; Zhang, J.; Wang, Z.; Xia, H.; Matyjaszewski, K. Temporal Control in Mechanically Controlled Atom Transfer Radical Polymerization Using Low ppm of Cu Catalyst. ACS Macro Lett. 2017, 6, 546–549.
- (47) Bandara, J.; Udawatta, C. P. K.; Rajapakse, C. S. K. Highly stable CuO incorporated TiO₂ catalyst for photocatalytic hydrogen production from H₂O. *Photochem. Photobiol. Sci.* **2005**, *4*, 857–861.
- (48) Saravanan, R.; Karthikeyan, S.; Gupta, V. K.; Sekaran, G.; Narayanan, V.; Stephen, A. Enhanced photocatalytic activity of ZnO/CuO nanocomposite for the degradation of textile dye on visible light illumination. *Mater. Sci. Eng.*, C 2013, 33, 91–98.
- (49) Wang, L.; Kang, Y.; Wang, Y.; Zhu, B.; Zhang, S.; Huang, W.; Wang, S. CuO nanoparticle decorated ZnO nanorod sensor for low-temperature H2S detection. *Mater. Sci. Eng., C* 2012, 32, 2079–2085.
- (50) Wang, B.; Durantini, J.; Nie, J.; Lanterna, A. E.; Scaiano, J. C. Heterogeneous Photocatalytic Click Chemistry. *J. Am. Chem. Soc.* **2016**, *138*, 13127–13130.
- (51) Xia, J.; Matyjaszewski, K. Controlled/"Living" Radical Polymerization. Atom Transfer Radical Polymerization Catalyzed by Copper(I) and Picolylamine Complexes. *Macromolecules* **1999**, 32, 2434–2437.
- (52) Yan, J.; Pan, X.; Wang, Z.; Lu, Z.; Wang, Y.; Liu, L.; Zhang, J.; Ho, C.; Bockstaller, M. R.; Matyjaszewski, K. A Fatty Acid-Inspired Tetherable Initiator for Surface-Initiated Atom Transfer Radical Polymerization. *Chem. Mater.* **2017**, *29*, 4963–4969.
- (53) Wang, Z.; Mahoney, C.; Yan, J.; Lu, Z.; Ferebee, R.; Luo, D.; Bockstaller, M. R.; Matyjaszewski, K. Preparation of Well-Defined Poly(styrene-co-acrylonitrile)/ZnO Hybrid Nanoparticles by an Efficient Ligand Exchange Strategy. *Langmuir* **2016**, *32*, 13207–13213.
- (54) Wang, X.; Song, J.; Liu, J.; Wang, Z. L. Direct-Current Nanogenerator Driven by Ultrasonic Waves. *Science* **2007**, *316*, 102–105
- (55) Cha, S. N.; Seo, J.-S.; Kim, S. M.; Kim, H. J.; Park, Y. J.; Kim, S.-W.; Kim, J. M. Sound-Driven Piezoelectric Nanowire-Based Nanogenerators. *Adv. Mater.* **2010**, *22*, 4726–4730.
- (56) Hong, K.-S.; Xu, H.; Konishi, H.; Li, X. Direct Water Splitting Through Vibrating Piezoelectric Microfibers in Water. *J. Phys. Chem. Lett.* **2010**, *1*, 997–1002.
- (57) Xu, Y.; Schoonen, M. A. A. The absolute energy positions of conduction and valence bands of selected semiconducting minerals. *Am. Mineral.* **2000**, *85*, 543–556.
- (58) Nanda, A. K.; Matyjaszewski, K. Effect of Penultimate Unit on the Activation Process in ATRP. *Macromolecules* **2003**, *36*, 8222–8224
- (59) Lin, C. Y.; Coote, M. L.; Petit, A.; Richard, P.; Poli, R.; Matyjaszewski, K. Ab Initio Study of the Penultimate Effect for the ATRP Activation Step Using Propylene, Methyl Acrylate, and Methyl Methacrylate Monomers. *Macromolecules* **2007**, *40*, 5985–5994.
- (60) Bravin, C.; Badetti, E.; Scaramuzzo, F. A.; Licini, G.; Zonta, C. Triggering Assembly and Disassembly of a Supramolecular Cage. *J. Am. Chem. Soc.* **2017**, *139*, 6456–6460.
- (61) Kruus, P.; Patraboy, T. J. Initiation of polymerization with ultrasound in methyl methacrylate. *J. Phys. Chem.* **1985**, *89*, 3379–3384.

(62) Price, G. J.; Norris, D. J.; West, P. J. Polymerization of methyl methacrylate initiated by ultrasound. *Macromolecules* **1992**, 25, 6447–6454

- (63) Xia, H.; Wang, Q.; Liao, Y.; Xu, X.; Baxter, S. M.; Slone, R. V.; Wu, S.; Swift, G.; Westmoreland, D. G. Polymerization rate and mechanism of ultrasonically initiated emulsion polymerization of n-butyl acrylate. *Ultrason. Sonochem.* **2002**, *9*, 151–158.
- (64) Lanzalaco, S.; Fantin, M.; Scialdone, O.; Galia, A.; Isse, A. A.; Gennaro, A.; Matyjaszewski, K. Atom Transfer Radical Polymerization with Different Halides (F, Cl, Br, and I): Is the Process "Living" in the Presence of Fluorinated Initiators? *Macromolecules* **2017**, *50*, 192–202.